



Contents lists available at ScienceDirect

Biochemical and Biophysical Research Communications

journal homepage: www.elsevier.com/locate/ybbrc



Importance of phospholipid bilayer integrity in the analysis of protein–lipid interactions



Patrick Drücker^a, Volker Gerke^b, Hans-Joachim Galla^{a,*}

^a Institute of Biochemistry, University of Münster, Wilhelm-Klemm-Str. 2, D-48149 Münster, Germany

^b Institute of Medical Biochemistry, ZMBE, University of Münster, Von-Esmarch-Str. 56, D-48149 Münster, Germany

ARTICLE INFO

Article history:

Received 10 September 2014

Available online 27 September 2014

Keywords:

Cholesterol
Phosphatidylinositol-(4,5)-bisphosphate (PIP₂, PI(4,5)P₂)
Solid supported bilayer
Lipid protein interactions

ABSTRACT

The integrity of supported phospholipid bilayer membranes is of crucial importance for the investigation of lipid–protein interactions. Therefore we recorded the formation of supported membranes on SiO₂ and mica by quartz crystal microbalance and controlled the integrity by atomic force microscopy. This study aims to analyze how membrane defects affect protein–lipid interactions. The experiments focused on a lipid mixture of POPC/DOPC/Chol/POPS/PI(4,5)P₂ (37:20:20:20:3) and the binding of the peripheral membrane associated protein annexin A2. We found that formation of a continuous undisturbed bilayer is an indispensable precondition for a reliable determination and quantification of lipid–protein-interactions. If membrane defects were present, protein adsorption causes membrane disruption and lipid detachment on a support thus leading to false determination of binding constants. Our results obtained for PI(4,5)P₂ and cholesterol containing supported membranes yield new knowledge to construct functional surfaces that may cover nanoporous substrates, form free standing membranes or may be used for lab-on-a-chip applications.

© 2014 Elsevier Inc. All rights reserved.

1. Introduction

Supported phospholipid membranes have been used for versatile applications, such as phase separation studies of lipids [1] and/or the characterization of protein adsorption. The apoptosis marker annexin A5 [2,3] or streptavidin, a protein often employed in biosensor applications [4,5], have been frequently considered to investigate lipid–protein-interactions at membrane surfaces.

Important for these investigations is the lipid mixture, which should resemble to some extent the natural composition of a biological membrane. In vertebrates, the plasma membrane contains significant levels of negatively charged lipids, such as phosphatidylserines (PS), furthermore the phosphatidylcholines (PC), about 30–40% cholesterol and ~1% phosphatidylinositol-(4,5)-bisphosphate (PI(4,5)P₂) [6–10]. Thus we used a lipid mixture of POPC/DOPC/Chol/POPS/PI(4,5)P₂ (37:20:20:20:3), which contains a high degree of *unsaturated* lipid acyl chains, mimicking the fluid nature of cellular membranes [11]. Solid supported bilayers (SLBs) form in several steps from vesicles and contain a variable water hydration

layer of 1–2 nm thickness between membrane and support (see review by Castellana et al. [12]). The formation of a PI(4,5)P₂ containing supported bilayer proceeds significantly faster and more reliable, when a buffer of low pH is used to minimize SUV surface charge [13,14]. However, a mixture containing both, PI(4,5)P₂ and cholesterol was not characterized in detail yet. Previous work applied the peripheral membrane associated protein annexin A5 to mechanically stabilize a lipid monolayer [15]. We here apply another member of the annexin protein family, annexin A2 or AnxA2 to probe lipid bilayer stabilization and to characterize the adsorption behavior.

Such a characterization of supported lipid bilayers is important for biosensor applications [16] using nanoporous substrates [17], protein nanopores [18] or nano-chip based sensors [19,20]. Furthermore, phospholipid bilayers of complex composition may be a target for drug screening on nanopores employing for example protein channels or blood brain barrier (BBB) membrane transporters like the ABC-transporter [21].

2. Materials and methods

2.1. Materials

The lipids, 1-palmitoyl-2-oleoyl-*sn*-glycero-3-phospho-L-serine (sodium salt) (POPS), 1,2-dioleoyl-*sn*-glycero-3 [phosphoinositol-

Abbreviations: SUV, small unilamellar vesicles; SLB, supported lipid bilayer; AnxA2, annexin A2; A2t, (AnxA2-S100A10)₂; AFM, atomic force microscopy; QCM-D, quartz crystal microbalance with dissipation monitoring.

* Corresponding author.

E-mail address: gallah@uni-muenster.de (H.-J. Galla).

4,5-bisphosphate] (triammonium salt) (PI(4,5)P₂), 1-palmitoyl-2-oleoyl-*sn*-glycero-3-phosphocholine (POPC), 1,2-dioleoyl-*sn*-glycero-3-phosphocholine (DOPC) were supplied by Avanti Polar Lipids Inc. (Alabaster, USA). Cholesterol was purchased from Sigma-Aldrich Life Science (Munich, Germany). HBS buffer contained 10 mM HEPES, 150 mM NaCl, pH 7.4. Citrate buffer contained 10 mM trisodiumcitrate, 150 mM NaCl and was adjusted to pH 4.6.

2.2. Vesicle preparation

Lipids and cholesterol stocks were dissolved in chloroform/methanol (1:1, v/v) (except PI(4,5)P₂; it was dissolved in chloroform/methanol/water, 20:9:1, v/v). After preparation of the lipid mixture, solvents were removed at 50 °C under a stream of nitrogen and thoroughly dried in vacuum overnight at 50 °C. Lipid films were suspended in the citrate buffer at 50 °C for 30 min with subsequent vortexing every 5 min. The resulting multilamellar vesicles were extruded 31 times through a polycarbonate membrane with 50 nm pore size at 50 °C (Avestin Liposofast, Ottawa, Canada).

2.3. Preparation of solid supported membranes

SiO₂ surfaces were cleaned and hydrophilized by 10 min UV/Ozone treatment, 30 min rinsing in 2% (w/v) SDS, 10 min UV/Ozone treatment and finally 3 min O₂-plasma treatment (Harrick Plasma, Ithaca, USA), subsequently rinsed with ultra pure water and dried under a stream of nitrogen. Mica was freshly cleaved before use. Then small unilamellar vesicles (0.1–0.2 mg/ml, 50 nm) were incubated at $T > T_{m, lipid}$ on the support. After bilayer preparation, the citrate buffer was exchanged by HBS pH 7.4.

2.4. QCM measurements

QCM experiments employed Q-Sense E4 QCM-D at 20 °C (Q-Sense, Gothenburg, Sweden). The flow chambers were connected to a peristaltic pump (Ismatec IPC, Glattbrugg, Switzerland) using a flow rate of 80.4 µl/min. Frequency and dissipation shifts of the 7th overtone resonance frequency of the sensor (QSX 303, 50 nm SiO₂, 5 MHz) were recorded.

2.5. AFM measurements

AFM employed a NanoWizard® 3 BioScience AFM (JPK Instruments AG, Berlin, Germany) on a Zeiss Axio Observer D.1 (Carl Zeiss AG, Oberkochen, Germany). For data analysis the JPK data processing software and Gwyddion were used. Intermittent contact measurements were done at 1 Hz line rate using MSCT cantilever with a nominal spring constant of 0.03–0.1 N/m and a silicon nitride tip. For calibration, thermal noise measurements were used. The force curve tip velocity was 0.5 µm/s. The scratching experiment was performed in contact mode at a line rate of 10 Hz with an increased set point, repeated 5 times.

2.6. Protein purification

AnxA2 and A2t were expressed and purified following a modified protocol from Nazmi et al. [22] as described [11].

3. Results

The deposition and formation of supported membranes on a SiO₂ substrate was monitored using the quartz crystal microbalance technique. The measured frequency shift ($\Delta F = F(t) - F_0$) is proportional to the adsorbed mass on the sensor surface [23,24] and the change in dissipation ($\Delta D = D(t) - D_0$) is an indicator of

the viscoelastic properties of the adsorbed layer or adlayer [24–26]. The formation of a supported bilayer involves several steps from vesicle adsorption, flattening, rupture and/or fusion and finally the formation of the bilayer [12]. Bilayers fabricated from simple lipid mixtures and their analyses by QCM have been described in detail [27,28]. Lipid mixtures containing negatively charged lipids like PI(4,5)P₂ or the combination of PI(4,5)P₂ and cholesterol can rapidly form bilayers, however only, if a buffer system with low pH is employed. This is more important than the use of bivalent ions like Ca²⁺ or Mg²⁺ to reduce vesicle repulsion and increase their surface affinity [13] (Drücker et al., submitted).

The formation of a POPC/DOPC/Chol/POPS/PI(4,5)P₂ (37:20:20:20:3) bilayer is shown in Fig. 1. When the sensor surface was equilibrated in 10 mM trisodiumcitrate, 150 mM NaCl, pH 4.6 (citrate buffer) (Fig. 1A, arrow A), the adsorption of the SUV suspension (arrow B) resulted in the formation of a stable membrane ($\Delta\Delta F = 29.4 \pm 0.4$ Hz, $\Delta\Delta D = 0.39 \pm 0.14 \cdot 10^{-6}$), which can be rinsed, HBS + 250 µM Ca²⁺ to raise the pH to physiological values (Fig. 1A, arrow C). This membrane may be further stabilized by protein adsorption. To study this we applied a peripheral membrane associated protein of the annexin family, the annexin A2 (AnxA2). This protein binds calcium dependently to negatively charged

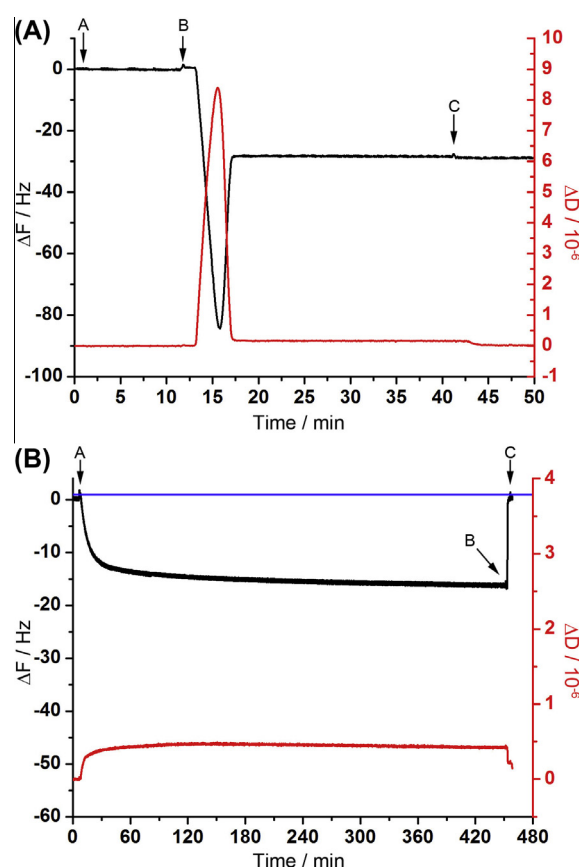


Fig. 1. Solid supported lipid bilayer covered by reversible protein adsorption. (A) Formation of a POPC/DOPC/Chol/POPS/PI(4,5)P₂ (37:20:20:20:3) solid supported bilayer. The clean SiO₂ surface is equilibrated in buffer (arrow A), before the SUV suspension is added (arrow B). Upon formation of a solid supported bilayer, the membrane was rinsed with HBS, pH 7.4 + 250 µM Ca²⁺ (arrow C). (B) Long term membrane coverage by adsorption of AnxA2. The addition of 50 nM AnxA2 in HBS + 250 µM Ca²⁺ leads to adsorption of a protein adlayer (arrow A). After addition of HBS + 2 mM EGTA, the protein adlayer can be reversibly removed (arrow B) and rinsed with new buffer e.g. HBS, pH 7.4 + 250 µM Ca²⁺ (arrow C). Note the reversible desorption of mass up to the original bilayer value (blue line). (For interpretation of the references to color in this figure legend, the reader is referred to the web version of this article.)

phospholipid membranes and can be reversibly removed by calcium-chelating agents [29–31]. The adsorption of 50 nM AnxA2 leads to the formation of a protein adlayer (Fig. 1B, arrow A), that was stable for several hours (Figs. 1A and S1) and could be reversibly removed by washing with HBS + 2 mM EGTA (Fig. 1B, arrow B). When the surface was washed subsequently with the buffer used before protein adsorption (HBS + 250 μ M Ca^{2+}), the original level of mass was restored (Fig. 1B, arrow C and blue line). Thus, after removal of the protein adlayer by Ca^{2+} chelating agents the membrane is again available for further interactions.

Next we applied atomic force microscopy to characterize the quality of the AnxA2 protein adlayer in a tapping mode. Topographical information of the specimen surface is obtained including information about the surface homogeneity from phase imaging. The AFM phase signals contain information about differences in Van der Waals-interaction-, solvation-, hydration-, electrostatic- or friction forces. Moreover, phase signals are affected by stiffness and mechanical parameters [32,33].

The adsorption of 50 nM AnxA2 on a POPC/DOPC/Chol/POPS/PI(4,5) P_2 (37:20:20:20:3) membrane results in a flat and homogeneous surface within the resolution limit of our experiment (Fig. 2A). The phase signal image contains almost no contrast which supports the view of a homogeneous and closed adlayer (Fig. 2B). To probe for the mechanical stability of the adlayer, we employed force spectroscopy by measuring force-distance curves. Pera et al. characterized the appearance of a bilayer rupture event or “jump” caused by the cantilever tip penetrating the membrane [34]. It results in a prominent discontinuity in the force distance curve. The force distance curve of the AnxA2 adlayer is depicted in Fig. 2C showing no discontinuity until an applied force of 30 nN in the trace/tip-surface approaching part (black graph). Thus the layer was not penetrated or punctured by the cantilever tip. Thereby protein adsorption may function as tool to mechanically stabilize the SLB membrane. The red, retraction curve shows the small (≈ 2.5 nN) tip-surface adhesion force and no abrupt break

of surface contact is observable. The hysteresis between the trace and retrace curve indicates a compressible, partially inelastic surface and excludes the possibility of measuring a pure non-covered silicon surface (Fig. 2C).

Next, we compared these results with the characteristics of an exposed supported POPC/DOPC/Chol/POPS/PI(4,5) P_2 (37:20:20:20:3) membrane, rinsed with by HBS + 250 μ M Ca^{2+} . Both, the topographical and the phase image reveal again a homogeneous surface with similar flatness as compared to the protein covered bilayer (Fig. 2E and F). No indication of microdomains is observed in presence of 250 μ M calcium. Employing force distance spectroscopy reveals a prominent bilayer rupture event at a force of about ~ 8 nN, indicating mechanical instability of the non-protein coated membrane (Fig. 2G, arrow). The appearance of a “jump” is a clear indicator of a bilayer being present on the substrate [34,35]. Although bilayer coverage of the tip itself is possible and would also result in a jump on e.g. an uncovered substrate, this is very unlikely due to the high curvature of the tip point [32,34].

Upon addition of protein to fragmented bilayers or bilayers containing small defects we observed a different characteristic. A fragmented bilayer, as depicted in Fig. 3A with the corresponding differences in the phase signal shown in Fig. 3B, is well distinguishable from the substrate if the defects were large. The height of a typical POPC/DOPC/Chol/POPS/PI(4,5) P_2 (37:20:20:20:3) bilayer patch on mica is 5.4 ± 0.1 nm. When protein is adsorbed, the shape of patches and the structure of layers differ significantly from adsorption on a complete bilayer. Fig. 3D shows the result of the incubation with a 100 nM solution of A2t, a complex form of AnxA2, on a bilayer which contained defects. The appearance of the image is dominated by a large number of small patches showing a disruption of the membrane caused by protein adsorption.

Richter et al. previously showed, that by scanning the surface with the cantilever tip, a merging of patches could be induced [36]. However, the cantilever tip did not induce such an assembly or merging of bilayer patches in the presence of A2t (Fig. 3D and E).

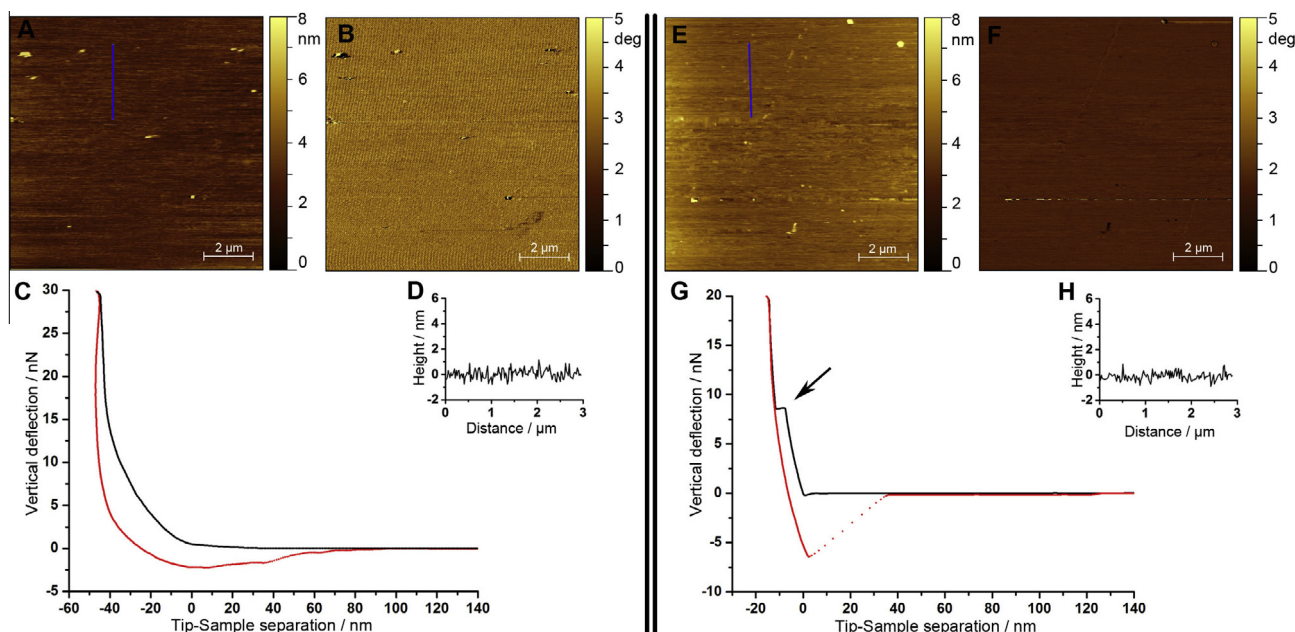


Fig. 2. SLB protection employing AnxA2 adsorption. (A) A POPC/DOPC/Chol/POPS/PI(4,5) P_2 (37:20:20:20:3) solid supported bilayer (SLB) was prepared on SiO_2 , gently rinsed with HBS + 250 μ M Ca^{2+} and incubated with 50 nM AnxA2 for 60 min at 20 °C. (B) Phase image of A. (C) Force distance curve on the protein adlayer presented in A. Note the high force without indication of a rupture event. (D) Corresponding height profile of the blue line in A. Note that the topographical image, phase image and line profile show a homogeneous and flat surface. (E) A POPC/DOPC/Chol/POPS/PI(4,5) P_2 (37:20:20:20:3) SLB was prepared on SiO_2 , gently rinsed with HBS + 250 μ M Ca^{2+} and analyzed. (F) Phase image of E. (G) Force distance curve on the POPC/DOPC/Chol/POPS/PI(4,5) P_2 (37:20:20:20:3) SLB on SiO_2 . Note the bilayer rupture event highlighted by the arrow and the high retraction force, necessary to break tip-support contact. Trace: black graph, retrace: red. (H) Corresponding height profile of the blue line in E. Note that the topographical image, phase image and line profile show again a homogeneous and flat surface. (For interpretation of the references to color in this figure legend, the reader is referred to the web version of this article.)

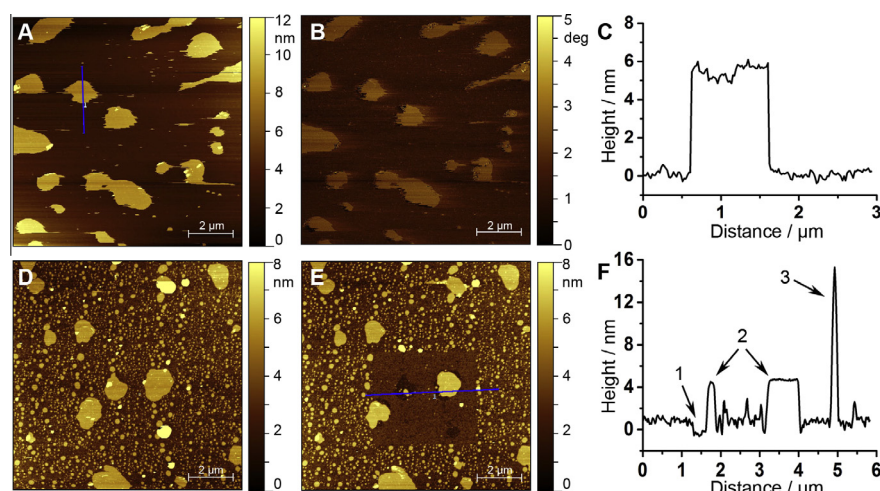


Fig. 3. Incomplete SLB and bilayer displacement. (A) A POPC/DOPC/Chol/POPS/PI(4,5)P₂ (37:20:20:20:3) fragmentary bilayer on mica (topographical image). (B) Corresponding phase image. (C) Height profile of a bilayer patch indicated by the blue line in A. The patch height is 5.4 ± 0.1 nm. (D) A POPC/DOPC/Chol/POPS/PI(4,5)P₂ (37:20:20:20:3) fragmentary bilayer prepared on mica, gently rinsed with HBS + 250 μ M Ca²⁺ and incubated with 100 nM A2t for 20 min at 20 °C. (E) Scratching on the bilayer depicted in D. An area of 4×4 μ m was scratched with the tip, 5 times at 10 Hz line rate in contact mode with higher force. (F) Height profile of the blue line in E. Arrow 1 marks the lowest level underneath a previous patch. Arrow 2 marks residual bilayer patches and arrow 3 indicates significantly higher structures. (For interpretation of the references to color in this figure legend, the reader is referred to the web version of this article.)

To analyze whether patches were in direct contact with the support or were embedded by surrounding protein, we scratched an area of 4×4 μ m on the surface via scanning in contact mode employing enhanced force and an increased line rate of 10 Hz with five repetitions (Fig. 3E). The majority of lipid patches and especially small bilayer patches could be removed from the surface. The lowest height in the image was observed in areas exposed underneath a previously large bilayer patch. The residual background area reveals a step height of ~ 1.8 nm related to the lowest observed level. The corresponding height profile is presented in Fig. 3F. Here mainly four steps in height could be distinguished: (1) the lowest level depicted by arrow 1, (2) the residual background, (3) residual bilayer patches (arrow 2) and (4) significantly higher structures (arrow 3). Further, the surface of bilayer patches appeared more flat than the possible protein background. Thus it appears that some bilayer patches, which could be removed, were not previously in direct contact with the substrate. Further it seems likely, that the background originates from protein adsorbed directly to the mica indicating that attractive forces of protein to the support were larger than the interaction of the SLB with the support. Bare mica sheets did not contain small areas of lower height levels and areas containing different layers of mica were not included in the analysis. Additionally, no protein could be identified on the residual bilayer patches, which could mean, that a higher attraction to the mica compared to the membrane was observed. Additionally, after the incubation of A2t, we could observe structures which were significantly higher than the membrane itself (Fig. 3F, arrow 3). These structures possibly result from bilayer patches which are displaced from the support and form vesicles or larger aggregates. Moreover, unspecific adsorption of AnxA2 could be observed on a SiO₂ support as well. Here only minor parts of AnxA2 ($\approx 10\%$) showed irreversible attraction to the support (Fig. S2).

4. Discussion

The formation of supported lipid bilayers, which contain large amounts of negatively charged lipids, may be difficult. Richter et al. previously reported, that a lipid membrane containing 50% PS did not form a proper bilayer [37]. Here we used a system containing 20% PS and 3% di-oleoyl-phosphatidylinositol-(4,5)-bisphosphate. The latter lipid contains a negative charge of 4 at

physiological pH of 7.4 [9,38,39]. Thus, the overall surface charge of SUVs composed of POPC/DOPC/Chol/POPS/PI(4,5)P₂ (37:20:20:20:3) is very high, which may hinder vesicle adsorption or rupture on a support. However, we could establish a suitable buffer system for the formation of PI(4,5)P₂ and cholesterol containing supported bilayers. The adsorption of a membrane binding protein, such as annexin A2, can be used to investigate biophysical interaction parameters like dissociation constants or cooperativity of lipid binding. Thus we analyzed the adsorption of A2t, the membrane associated complex of AnxA2 [31].

During the preparation of solid supported bilayers for lipid–protein interaction investigations, defects in the membrane may occur and are difficult to identify. Richter et al. reported previously, that DOPC/DOPS (4:1) bilayers contained small, almost invisible defects identified by atomic force microscopy [36]. We here present an example, where a fragmented or even defect bilayer has severe impact on protein adsorption studies. Minor defects in the SLB dramatically affected the bilayer stability if the peripheral membrane binding annexin A2 was adsorbed on mica which resulted in layer instability and eventual lipid displacement. We observed that the protein exhibited stronger affinity to a mica support as compared to the supported membrane itself. This resulted in displacement of lipids from the support and protein could also be found underneath bilayer patches. When protein adsorption experiments revealed a flat and homogeneous surface, where a bilayer-bound protein adlayer was difficult to distinguish from a complete and homogeneous bilayer alone, the application of force distance curves was a valuable tool [40] to differentiate. Firstly, a bilayer shows a significant jump or bilayer rupture event, which resulted from the penetration with the cantilever tip and further the retract part of a force distance curve showed a certain retention force of more than 5 nN on mica, which broke abruptly in one step. Secondly, the protein adlayer was compressible and could appear inelastic, indicated by the prominent hysteresis between the trace and retrace part of the force curve. Also the retention force was smaller and a longer tip–adlayer interaction was observed as no abrupt contact loss appeared.

A SiO₂ support exhibits increased lipid mobility as compared to mica [1]. Thus it will affect protein–lipid interaction studies where lipids may be recruited into domains. The integrity of supported bilayers is crucial for protein–lipid interaction studies. On the other hand, a long-term and reversible protein adsorption results

in bilayer stabilization and protection from mechanical stress. The stabilization of a Langmuir–Blodgett transferred lipid monolayer following the adsorption of annexin A5 was shown by Simon et al. [15]. Here we used annexin A2 to mechanically stabilize a supported bilayer system of complex composition, mimicking to some extent the content of cellular membranes. This stabilization was verified employing force distance curves, revealing that an annexin A2 covered bilayer cannot be penetrated by the tip at forces that would penetrate the uncovered bilayer alone. The adlayer showed no rupture event until a force of 30 nN affecting an area of ~ 10 nm in diameter (size of tip point). Successful protein deposition and long-term mechanical stability of $\text{PI}(4,5)\text{P}_2$ and cholesterol containing continuous supported membranes were established by adsorption of annexin A2. These membranes were reliably used in QCM-measurements showing that they are applicable for further biosensor applications.

Acknowledgments

We thank Dr. Milena Pejic for supplying purified A2t and Jasmin Halle and Eva Kolbeck for their skillful contribution within a lab research course. This work was supported by the German Research Council (DFG) – SFB 858, project B4.

Appendix A. Supplementary data

Supplementary data associated with this article can be found, in the online version, at <http://dx.doi.org/10.1016/j.bbrc.2014.09.079>.

References

- [1] H.M. Seeger, A.D. Cerbo, A. Alessandrini, P. Facci, Supported lipid bilayers on mica and silicon oxide: comparison of the main phase transition behavior, *J. Phys. Chem. B* 114 (2010) 8926.
- [2] R.P. Richter, A. Brisson, Characterization of lipid bilayers and protein assemblies supported on rough surfaces by atomic force microscopy, *Langmuir* 19 (2003) 1632.
- [3] C. Janko, J. Ivica, B. Mona, C. Ricardo, S. Christine, E.M. Luis, H. Martin, Cooperative binding of annexin A5 to phosphatidylserine on apoptotic cell membranes, *Phys. Biol.* 10 (2013) 65006.
- [4] P. Seelheim, H.-J. Galla, Tethered proteoliposomes containing human ABC transporter MRP3: new perspectives for biosensor application based on transmembrane proteins, *Biochem. Biophys. Res. Commun.* 431 (2013) 519.
- [5] O. Roling, C. Wendeln, U. Kauscher, P. Seelheim, H.-J. Galla, B.J. Ravoo, Layer-by-layer deposition of vesicles mediated by supramolecular interactions, *Langmuir* 29 (2013) 10174.
- [6] V. Kiessling, C. Wan, L.K. Tamm, Domain coupling in asymmetric lipid bilayers, *Biochim. Biophys. Acta* 1788 (2009) 64.
- [7] G. van Meer, D.R. Voelker, G.W. Feigenson, Membrane lipids: where they are and how they behave, *Nat. Rev. Mol. Cell Biol.* 9 (2008) 112.
- [8] T.P.W. McMullen, R.N.A.H. Lewis, R.N. McElhaney, Cholesterol–phospholipid interactions, the liquid-ordered phase and lipid rafts in model and biological membranes, *Curr. Opin. Colloid Interface Sci.* 8 (2004) 459.
- [9] S. McLaughlin, J. Wang, A. Gambhir, D. Murray, PIP_2 and proteins: interactions, organization, and information flow, *Annu. Rev. Biophys. Biomol.* 31 (2002) 151.
- [10] J. Wang, A. Gambhir, G. Hangyás-Mihályné, D. Murray, U. Golebiewska, S. McLaughlin, Lateral sequestration of phosphatidylinositol 4,5-bisphosphate by the basic effector domain of myristoylated alanine-rich C kinase substrate is due to nonspecific electrostatic interactions, *J. Biol. Chem.* 277 (2002) 34401.
- [11] P. Drücker, M. Pejic, H.-J. Galla, V. Gerke, Lipid segregation and membrane budding induced by the peripheral membrane binding protein annexin A2, *J. Biol. Chem.* 288 (2013) 24764.
- [12] E.T. Castellana, P.S. Cremer, Solid supported lipid bilayers: from biophysical studies to sensor design, *Surf. Sci. Rep.* 61 (2006) 429.
- [13] J.A. Braunger, C. Kramer, D. Morick, C. Steinem, Solid supported membranes doped with PIP_2 : influence of ionic strength and pH on bilayer formation and membrane organization, *Langmuir* 29 (2013) 14204.
- [14] M. Baumann, E. Amstad, A. Mashaghi, M. Textor, E. Reimhult, Characterization of supported lipid bilayers incorporating and phosphoinositol-3,4,5-triphosphate by complementary techniques, *Biointerphases* 5 (2010) 114.
- [15] A. Simon, C. Gounou, S. Tan, L. Tiefenauer, M. Di Berardino, A.R. Brisson, Free-standing lipid films stabilized by annexin-A5, *Biochim. Biophys. Acta* 1828 (2013) 2739.
- [16] E. Reimhult, K. Kumar, Membrane biosensor platforms using nano- and microporous supports, *Trends Biotechnol.* 26 (2008) 82.
- [17] M. Urban, A. Kleefen, N. Mukherjee, P. Seelheim, B. Windschiegl, M. Vor der Brüggen, A. Koçer, R. Tampé, Highly parallel transport recordings on a membrane-on-nanopore chip at single molecule resolution, *Nano Lett.* 14 (2014) 1674.
- [18] T. Zhuang, L.K. Tamm, Control of the conductance of engineered protein nanopores through concerted loop motions, *Angew. Chem. Int. Ed.* 53 (2014) 5897.
- [19] C. Schmidt, M. Mayer, H. Vogel, A chip-based biosensor for the functional analysis of single ion channels, *Angew. Chem. Int. Ed.* 39 (2000) 3137.
- [20] L. Galla, A.J. Meyer, A. Spiering, A. Sischka, M. Mayer, A.R. Hall, P. Reimann, D. Anselmetti, Hydrodynamic slip on DNA observed by optical tweezers-controlled translocation experiments with solid-state and lipid-coated nanopores, *Nano Lett.* 14 (2014) 4176.
- [21] P. Seelheim, A. Wüllner, H.-J. Galla, Substrate translocation and stimulated ATP hydrolysis of human ABC transporter MRP3 show positive cooperativity and are half-coupled, *Biophys. Chem.* 171 (2013) 31.
- [22] R. Nazmi Ali, G. Ozorowski, M. Pejic, P. Whitelegge Julian, V. Gerke, H. Luecke, N-terminal acetylation of annexin A2 is required for S100A10 binding, *Biol. Chem.* 393 (2012) 1141.
- [23] G. Sauerbrey, Verwendung von schwingquarzen zur wägung dünner schichten und zur mikrowägung, *Z. Phys. A: Hadrons Nucl.* 155 (1959) 206.
- [24] A. Janshoff, H.-J. Galla, C. Steinem, Piezoelectric mass-sensing devices as biosensors – an alternative to optical biosensors?, *Angew. Chem. Int. Ed.* 39 (2000) 4004.
- [25] J. Fattison, F. Azari, N. Tufenkji, Real-time QCM-D monitoring of cellular responses to different cytomorphic agents, *Biosens. Bioelectron.* 26 (2011) 3207.
- [26] M. Rodahl, F. Höök, B. Kasemo, QCM operation in liquids: an explanation of measured variations in frequency and Q factor with liquid conductivity, *Anal. Chem.* 68 (1996) 2219.
- [27] R. Richter, A. Mukhopadhyay, A. Brisson, Pathways of lipid vesicle deposition on solid surfaces: a combined QCM-D and AFM study, *Biophys. J.* 85 (2003) 3035.
- [28] E. Reimhult, F. Höök, B. Kasemo, Vesicle adsorption on SiO_2 and TiO_2 : dependence on vesicle size, *J. Chem. Phys.* 117 (2002) 7401.
- [29] M. Ross, V. Gerke, C. Steinem, Membrane composition affects the reversibility of annexin A2t binding to solid supported membranes: a QCM study, *Biochemistry* 42 (2003) 3131.
- [30] V. Gerke, C.E. Creutz, S.E. Moss, Annexins: linking Ca^{2+} signalling to membrane dynamics, *Nat. Rev. Mol. Cell Biol.* 6 (2005) 449.
- [31] V. Gerke, S.E. Moss, Annexins: from structure to function, *Phys. Rev.* 82 (2002) 331.
- [32] Z. Leonenko, D.T. Cramb, M. Amrein, E. Finot, Atomic force microscopy: Interaction forces measured in phospholipid monolayers, bilayers and cell membranes, in: M. Tomitori, B. Bhushan, H. Fuchs (Eds.), *Applied Scanning Probe Methods IX*, Springer, Berlin, Heidelberg, 2008, p. 207.
- [33] H.-J. Butt, B. Cappella, M. Kappl, Force measurements with the atomic force microscope: technique, interpretation and applications, *Surf. Sci. Rep.* 59 (2005) 1.
- [34] I. Pera, R. Stark, M. Kappl, H.-J. Butt, F. Benfenati, Using the atomic force microscope to study the interaction between two solid supported lipid bilayers and the influence of synapsin I, *Biophys. J.* 87 (2004) 2446.
- [35] S. Garcia-Manyes, F. Sanz, Nanomechanics of lipid bilayers by force spectroscopy with AFM: a perspective, *Biochim. Biophys. Acta* 1798 (2010) 741.
- [36] R.P. Richter, A.R. Brisson, Following the formation of supported lipid bilayers on mica: a study combining AFM, QCM-D, and ellipsometry, *Biophys. J.* 88 (2005) 3422.
- [37] R.P. Richter, R. Bérat, A.R. Brisson, Formation of solid-supported lipid bilayers: an integrated view, *Langmuir* 22 (2006) 3497.
- [38] Z.T. Graber, A. Gericke, E.E. Kooijman, Phosphatidylinositol-4,5-bisphosphate ionization in the presence of cholesterol, calcium or magnesium ions, *Chem. Phys. Lipids* 182 (2014) 62.
- [39] Z.T. Graber, Z. Jiang, A. Gericke, E.E. Kooijman, Phosphatidylinositol-4,5-bisphosphate ionization and domain formation in the presence of lipids with hydrogen bond donor capabilities, *Chem. Phys. Lipids* 165 (2012) 696.
- [40] C. Canale, M. Jacono, A. Diaspro, S. Dante, Force spectroscopy as a tool to investigate the properties of supported lipid membranes, *Microsc. Res. Tech.* 73 (2010) 965.